Chemical Physics Letters 482 (2009) 38–43

Contents lists available at ScienceDirect

Chemical Physics Letters

journal homepage: www.elsevier.com/locate/cplett

Photophysics of the Trp-Gly dipeptide: Role of electron and proton transfer processes for efficient excited-state deactivation

Dorit Shemesh [a,*], Christof Hättig [b], Wolfgang Domcke [a]

[a] Department of Chemistry, Technische Universität München, 85747 Garching, Germany
[b] Department of Chemistry, Ruhr-Universität Bochum, 44801 Bochum, Germany

ARTICLE INFO

Article history:
Received 5 August 2009
In final form 25 September 2009
Available online 30 September 2009

ABSTRACT

The excited-state potential-energy surfaces of the lowest-energy conformer of the tryptophan–glycine dipeptide have been investigated with ab initio electronic-structure methods. The calculations reveal a potentially very efficient excited-state deactivation mechanism via conical intersections of the excited states of the indole chromophore with locally-excited and charge-transfer states of the peptide backbone. These findings suggest that the excited-state lifetime of the lowest-energy conformer of the Trp-Gly dipeptide may be too short to allow the detection of a resonant two-photon ionization signal. It is proposed that the efficient excited-state deactivation enhances the photostability of the dipeptide.

© 2009 Elsevier B.V. All rights reserved.

1. Introduction

Amino acids are the elementary building blocks of peptides and proteins. Electrostatic interactions, hydrogen bonds and salt bridges stabilize the three-dimensional structure of proteins. In the last decade, a rapidly increasing number of experiments and theoretical calculations have been devoted to isolated small peptides, e.g. dipeptides and tripeptides, aiming at the understanding of the local structural preferences of particular amino acids [1–13]. These experiments provide detailed information on the structure and energetics of different conformers of small peptides and give insight into the driving forces for the formation of the secondary structure of peptides and proteins. Most of the spectroscopic studies are performed on protected peptides [1–4,6–8,10,13]. Different capping groups protect these peptides at their termini. These capping groups are chosen so that they do not to interfere with hydrogen bonding within the peptide backbone. Capped dipeptides and tripeptides serve therefore as models for the understanding of the generic structure of small segments of proteins.

Hydrogen bonds play an important role in stabilizing the secondary structure of peptides. The most common hydrogen bonds found in proteins are hydrogen bonds between the N–H group on one peptide bond and the O=C group of another peptide bond. Several structural motifs are found in proteins: The α-helix is built from a peptide strand where the *i*th residue is connected with the $(i+4)$th residue via a hydrogen bond between the N–H group and the C=O group. The β-sheet, on the other hand, is built from two strands of peptides aligned either parallel or antiparallel and stabilized by hydrogen-bond interactions between the N–H group of one strand and the C=O group of the other strand (and vice versa). Other important structural motifs are the β-turn and the γ-turn. The β-turn (γ-turn) is built from a hydrogen bond where the donor and acceptor residues are separated by 2 residues (3 residues). The H-bonding interaction is between the N–H group of one residue and the C=O group of the other residue. Most of these hydrogen bonds are moderately strong hydrogen bonds. The distance between the donor and the acceptor atoms is approximately 3 Å [14,15]. As a rule, the weakest hydrogen bond is found in β-sheets, followed by a slightly stronger hydrogen bond in the α-helix. β-Turns involve stronger hydrogen bonds than the hydrogen bonds encountered in α-helices. From all the hydrogen bonds mentioned so far, the γ-turns exhibit the strongest N–H···O–C interactions found in peptides. γ-turns are encountered frequently in short peptides [4]. We have recently investigated the photophysics of simple peptides exhibiting β-turns and the γ-turns [16,17]. Herein, we focus on the photoinduced proton-transfer process associated with a strong hydrogen bond generally found at the C-terminus of peptides.

Natural peptides terminate on one end with a free carboxylic group and on the other end with a free amino group. These groups can interact via hydrogen bonds with the peptide backbone. In this work, we have investigated the natural (uncapped) dipeptide tryptophan–glycine (Trp-Gly). The resonant multi-photon ionization (REMPI) spectrum of Trp-Gly and Trp-Gly-Gly was recorded recently [12]. This spectroscopic work was supported by a thorough theoretical exploration of the conformational space [5]. Unexpectedly, some of the energetically most stable conformers were not found in the REMPI spectra. The most stable conformers exhibit a strong hydrogen bond which connects the free carboxylic group on the C-terminus with the carbonyl group of the peptide bond, see the encircled region in Fig. 1. This hydrogen bond can be

* Corresponding author.
E-mail address: dorit.shemesh@ch.tum.de (D. Shemesh).

0009-2614/$ - see front matter © 2009 Elsevier B.V. All rights reserved.
doi:10.1016/j.cplett.2009.09.087

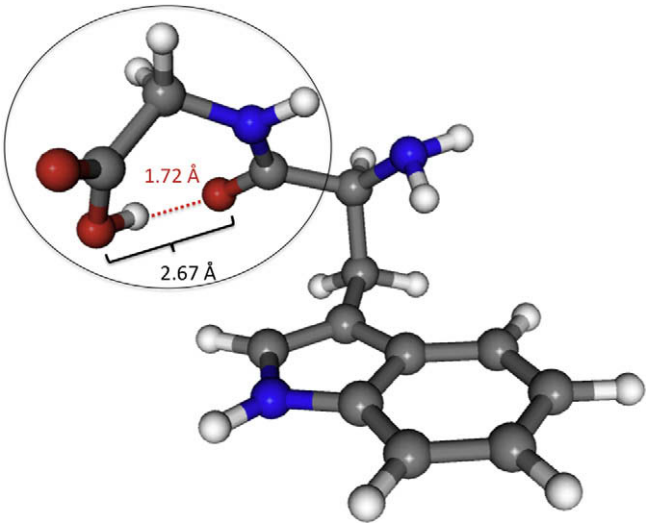


Fig. 1. MP2 ground-state equilibrium geometry of the conformer wg01[g+.0.70] of Trp-Gly. The ellipse encircles a hydrogen-bond motif which is commonly found in the backbone of uncapped peptides.

formed by every C-terminus in peptides. We concentrate here on the photophysics of the proton transfer along this hydrogen bond. We suggest that this strong hydrogen bond gives rise to an efficient excited-state deactivation mechanism for this particular conformer of Trp-Gly. Our results suggest that this efficient radiationless decay pathway is responsible for the absence of this conformer in the REMPI spectrum.

2. Computational methods

The ground-state equilibrium geometry of the conformer wg01[g+.0.70] (see Ref. [5]) of Trp-Gly has been determined with the second-order Møller–Plesset (MP2) method. Excitation energies have been calculated with the ADC(2) (algebraic diagrammatic construction through second order) method [18–22]. For comparison, the vertical excitation energies have also been calculated with the CC2 (approximate second-order coupled cluster) method [23,24]. The performance of ADC(2) compared with CC2 and related methods has thoroughly been investigated by Hättig [18]. The advantage of the ADC(2) method is that the excitation energies are calculated as the eigenvalues of a Hermitian secular matrix, while in coupled-cluster response theory they are obtained from a non-Hermitian Jacobi matrix. The ADC(2) method is therefore able to describe conical intersections between excited states physically correctly, which need not to be the case for coupled-cluster theory [25].

The equilibrium geometries and reaction paths of the excited singlet states have been determined at the ADC(2) level, making use of analytic ADC(2) gradients [18]. A relaxed scan for the transfer of the proton from the hydroxyl group to the carbonyl group has been computed: The OH bond length R_{OH} of the carboxyl group involved in the hydrogen bonding has been chosen as the driving coordinate of the reaction path; all other internal coordinates have been optimized, for a given value of R_{OH}, in the respective electronic state. When the calculation of a relaxed scan was not possible, a linearly interpolated transit path (LITP) has been calculated between educt and product geometries. Intermediate geometries were constructed by interpolating between the terminal geometries in internal coordinates. All calculations were carried out with the TURBOMOLE program suite [26], making use of the resolution-of-the-identity (RI) approximation for the evaluation of the electron-repulsion integrals [27]. The cc-pVDZ basis set has been employed throughout.

3. Results

3.1. Ground-state equilibrium structure

The structure of the conformer wg01[g+.0.70] of the Trp-Gly dipeptide is shown in Fig. 1. This conformer has been identified as the lowest enthalpy conformer by Valdes et al. [5]. This structure exhibits a hydrogen bond between the OH of the carboxyl group and the O=C of the nearest peptide bond ($O–H_{carb}\cdot\cdot O{=}C_{pep}$), see Fig. 1. This hydrogen bond also exists in other structures like wg02[t.140.-70] and wg03[g+.-20.70], see Ref. [5]. All of these conformers could not be identified in the REMPI spectrum [12]. The distance between the carboxylic hydrogen and the carbonyl oxygen is 1.72 Å. The distance between the two oxygens is 2.67 Å. According to established empirical rules, this distance corresponds to a strong hydrogen bond [28,29].

3.2. Excitation energies and molecular orbitals

The vertical excitation energies, dipole moments and oscillator strengths of the lowest two excited singlet states *of the chromophore* of conformer wg01[g+.0.70] of Trp-Gly are summarized in Table 1. The frontier molecular orbitals (MOs) are shown in Fig. 2. The lowest two excited singlet states of the indole chromophore are the well-known $^1L_b(\pi\pi^*)$ and $^1L_a(\pi\pi^*)$ states. The ADC(2) vertical excitation energies are 4.85 eV and 4.94 eV. CC2 gives very similar results: 4.87 eV and 4.93 eV. The lowest $^1\pi\pi^*$ excited state has an oscillator strength of 0.038, whereas the oscillator strength of the second state is 0.082. The dipole moment of the lowest excited state is 4.49 Debye, that of the second state is 4.18 Debye. The first excited state thus possesses the higher dipole moment, while the second excited state possesses the higher oscillator strength. On the basis of these properties, we tentatively assign the first excited state as the ^1L_b state and the second state as the ^1L_a state *at the ground-state equilibrium geometry.* Optimization of the lowest excited state *of the chromophore* yields an adiabatic excitation energy of about 3.63 (3.66) eV with ADC(2) (CC2). The oscillator strength of the lowest chromophore excited state at its optimized geometry is 0.073, compared to 0.0098 for the second state. The corresponding dipole moments are 5.73 Debye and 3.70 Debye. These properties clearly indicate that the lowest excited state *of the chromophore at its equilibrium geometry* is of ^1L_a character. The energetic ordering of the ^1L_b and ^1L_a states is thus reversed upon geometry optimization. The MOs associated with the next two excited singlet states are n-type or σ-type orbitals mainly located on the backbone of the dipeptide.

3.3. ^1L_b–^1L_a inversion in the Franck–Condon region

As discussed above, the first excited state at the ground-state equilibrium geometry is the ^1L_b state, whereas the ^1L_a state

Table 1
Vertical excitation energies (ΔE, in eV), oscillator strengths (f) and dipole moments (μ, in Debye) of Trp-Gly (conformer wg01[g+.0.70]), calculated with the ADC(2)/cc-pVDZ and CC2/cc-pVDZ methods at the MP2/cc-pVDZ equilibrium geometry.

State	CC2	ADC(2)		
	ΔE	ΔE	f	μ
$^1\pi\pi^*$ (^1L_b)	4.87	4.85	0.038	4.49
$^1\pi\pi^*$ (^1L_a)	4.93(3.66)[a]	4.94(3.63)[a]	0.082	4.18

[a] Adiabatic excitation energy.

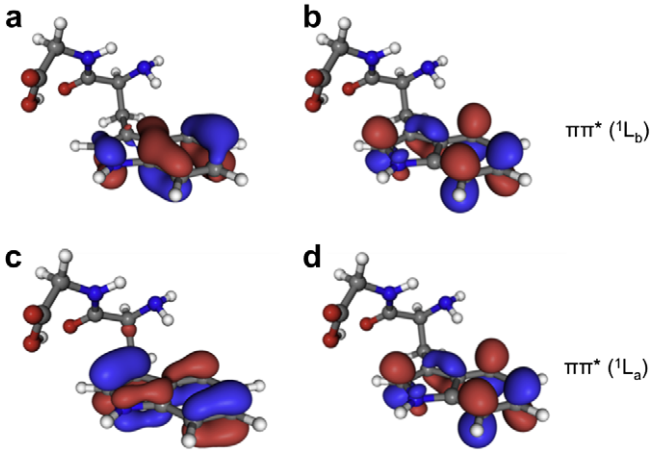


Fig. 2. Canonical Hartree–Fock orbitals of the chromophore of the wg[g+.0.70] conformer of Trp-Gly. (a) Occupied orbital of the ^1L_b state; (b) unoccupied orbital of the ^1L_b state; (c) occupied orbital of the ^1L_a state; (d) unoccupied orbital of the ^1L_a state. The ^1L_b state corresponds mainly (67%) to the excitation of an electron from (a) to (b); the ^1L_a state corresponds mainly (75%) to the excitation of an electron from (c) to (d).

becomes the lowest excited singlet state *of the indole chromophore* upon geometry optimization. We calculated the ^1L_b and ^1L_a energy profiles along the LITP connecting these two structures. The result is shown in Fig. 3. Along this path, the ^1L_a state is stabilized energetically, whereas the ^1L_b state rises in energy. The ^1L_a–^1L_b crossing occurs very close to the ground-state equilibrium geometry and is essentially isoenergetic with the vertical excitation energy of the ^1L_b state. The optimized energy of the ^1L_a state lies about 0.45 eV below the ^1L_a vertical excitation energy. The structural changes include variations in the bond lengths of the indole moiety as well as of the backbone. The five-membered and six-membered rings expand and the backbone moves nearer to the ring along the linear transit path.

For comparison, Table 2 gives the vertical excitation energies of the bare indole molecule. The ^1L_b state of indole has the same vertical excitation energy as the lowest excited state in Trp-Gly. The lower oscillator strength and dipole moment of the first excited state compared to the second excited state clearly identify it as

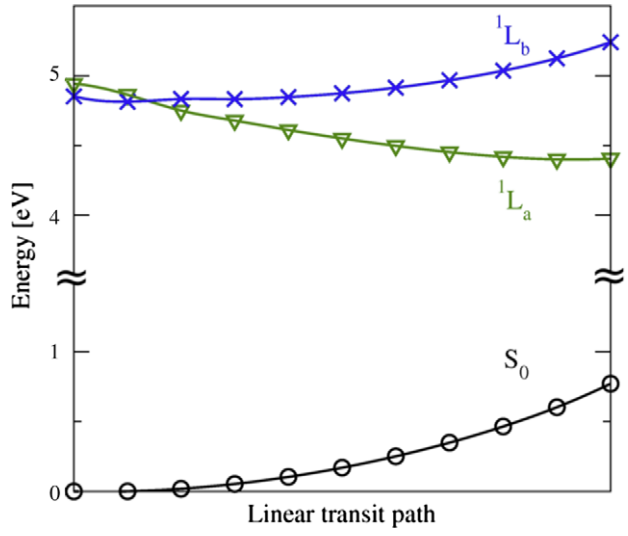


Fig. 3. Potential-energy profiles of the ^1L_a, ^1L_b and S_0 states along the linearly interpolated transit path between the S_0 minimum-energy geometry and the ^1L_a minimum-energy geometry.

Table 2
Vertical excitation energies (ΔE, in eV), oscillator strengths (f) and dipole moments (μ, in Debye) of indole, calculated with the ADC(2)/cc-pVDZ method at the MP2/cc-pVDZ equilibrium geometry.

State	ADC(2)		
	ΔE	f	μ
$^1\pi\pi^*$ (^1L_b)	4.87(4.87)[a]	0.035	2.55
$^1\pi\pi^*$ (^1L_a)	5.18	0.118	6.62

[a] Adiabatic excitation energy.

the ^1L_b state. The orbital characters of both excited states are similar to those of Trp-Gly. While the energy difference of both states is about 0.31 eV in indole, it is merely 0.09 eV in Trp-Gly. The lowering of the ^1L_a state relative to the ^1L_b states is well known for indole derivates in solution, there the ^1L_a state with the higher dipole moment experiences a larger stabilization than the ^1L_b state in polar solvents. It seems that the peptidic backbone in Trp-Gly has a similar effect on the ^1L_a state. The adjustment of the backbone can strongly stabilize the ^1L_a state. These findings are in agreement with experimental results of Zwier and collaborators. They have shown that the conformation of the polypeptide backbone has a significant effect on the relative energies of the ^1L_b and ^1L_a states. The ordering of the ^1L_b and ^1L_a states may differ for different conformers of the same molecule [30].

3.4. Proton-transfer reaction path

The energy profiles of the proton-transfer reaction path along the O–H···O=C hydrogen bond are depicted in Fig. 4a. The proton is transferred from the hydroxyl group of the carboxyl group to the carbonyl group along the hydrogen bond (see Fig. 1). All the symbols in the graph refer to optimized structures (with the constraint of a fixed OH distance); the lines are interpolations of these points. The $\pi\pi^*$ state (green) is denoted by top-down triangles, the locally excited state (^{1}LE, blue[1]) by squares, the charge-transfer state (^{1}CT, red) by top-up triangles and the ground state (black) by circles. $S_0^{(\pi\pi^*)}$ represents the ground-state energy calculated at the geometry of the $^1\pi\pi^*$ state, etc.

As discussed above, the lowest vertically excited state in the Franck–Condon region is the ^1L_b ($\pi\pi^*$) state. Geometry optimization of the lowest $\pi\pi^*$ excited state *of the indole chromophore* yields the ^1L_a ($\pi\pi^*$) state, see previous section. However, the excited state of Trp-Gly with the lowest adiabatic excitation energy is not the ^1L_a state, but a locally excited state *of the peptide group.* We refer to this state as ^{1}LE state. The half-filled molecular orbitals are depicted in Fig. 5a and b. It is seen that this electronic excitation is completely localized on the peptide backbone and the terminal groups. The geometric structure of Trp-Gly at the equilibrium geometry of the ^{1}LE state is very different from the ground-state equilibrium structure, as can be seen from the increase of the ground-state energy by more than 2 eV (see $S_0^{(LE)}$ curve in Fig 4a). Upon stretching of the OH distance, a charge-transfer state (^{1}CT) is strongly stabilized, see Fig. 4a. The corresponding molecular orbitals are shown in Fig. 5c and d. It is seen that in the ^{1}CT state one electronic charge unit is transferred from the terminal carboxyl group to the NH and CO groups of the backbone. Upon geometry optimization of the ^{1}CT state, the proton of the carboxyl group follows the electronic charge along the O–H···O hydrogen bond, resulting in a stabilization of the ^{1}CT state by several electron volts (see Fig. 4a). The result of this electron-driven proton-transfer (EDPT) process [16,31] is a biradical. The optimized geometric structure of the biradical is very different from the equilibrium

[1] For interpretation of color in Figs. 1–7, the reader is referred to the web version of this article.

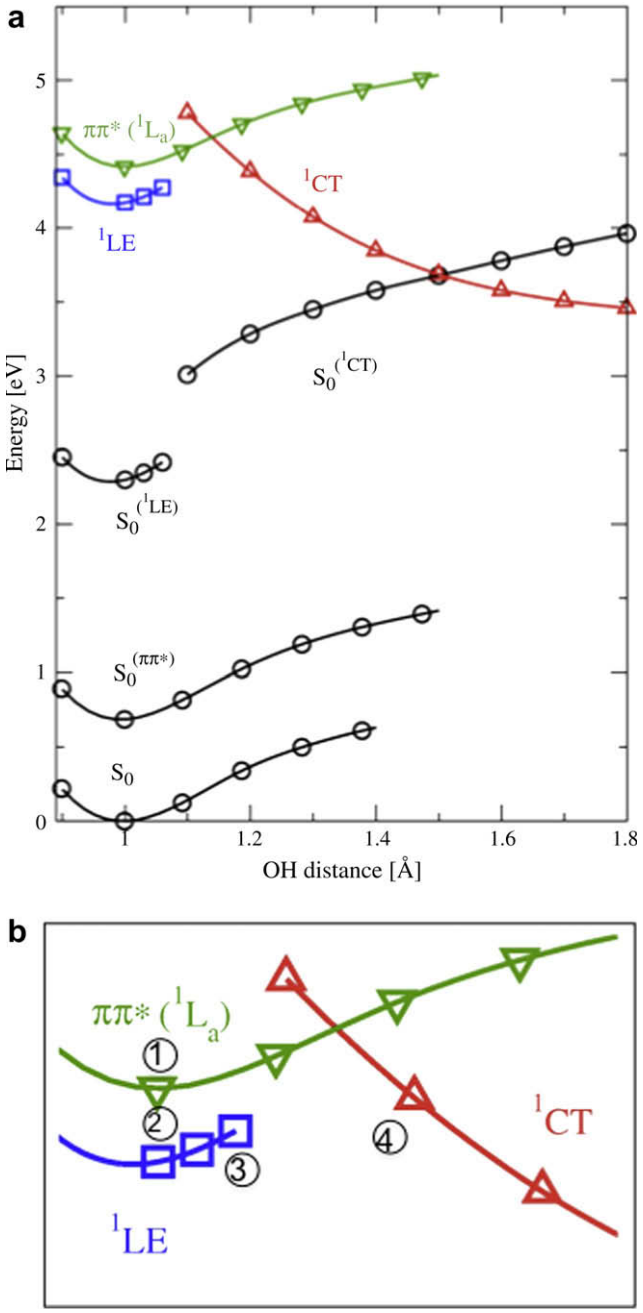


Fig. 4. (a) Minimum-energy profiles (relaxed scans) of the ^1L_a state (top-down triangles), the locally excited state, (^{1}LE, squares) and the charge-transfer state, (^{1}CT, top-up triangles) of Trp-Gly along the proton-transfer coordinate. The ^1L_a, ^{1}LE and ^{1}CT energies have been determined at the minimum-energy geometries of the respective state. The ground-state energies designated as S_0 have been calculated at the minimum-energy geometries of the S_0 state, while the S_0 energies designated as $S_0^{(CT)}$ have been determined at the minimum-energy geometries of the ^{1}CT state. (b) Enlargement of the excited-state energies near the Franck–Condon region. Corresponding LITPs are shown in Figs. 6 and 7.

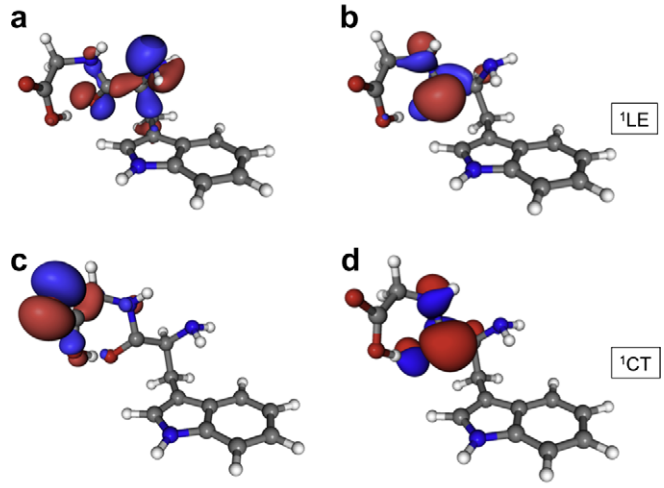


Fig. 5. Canonical Hartree–Fock orbitals of the backbone of the wg[g+.0.70] conformer of Trp-Gly. (a) Occupied orbital of the ^{1}LE state at R_{NH} = 1.06 Å; unoccupied orbital of the ^{1}LE state at R_{NH} = 1.06 Å; (c) occupied orbital of the ^{1}CT state at R_{NH} = 1.1 Å; (d) unoccupied orbital of the ^{1}CT state at R_{NH} = 1.1 Å. The ^{1}LE state corresponds mainly (48%) to the excitation of an electron from (a) to (b); the ^{1}CT state corresponds mainly (91%) to the excitation of an electron from (c) to (d).

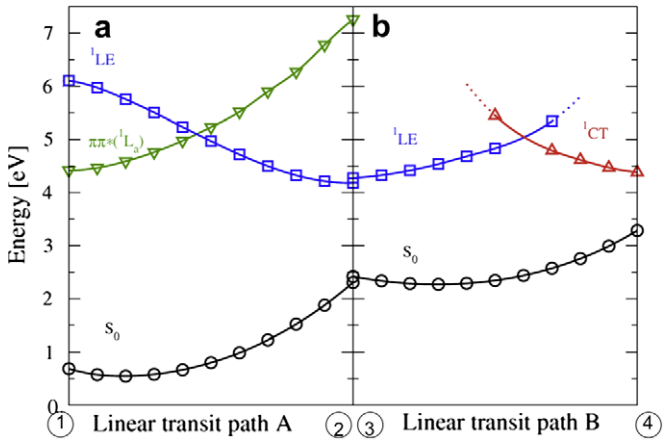


Fig. 6. (a) Potential-energy profiles of the ^1L_a, ^{1}LE and S_0 states along the linearly interpolated transit path between the ^1L_a minimum-energy geometry (structure 1) and the ^{1}LE minimum-energy geometry at R_{NH} = 1.0 Å (structure 2). (b) Potential-energy profiles of the ^{1}LE, ^{1}CT and S_0 states along the linearly interpolated transit path between the ^{1}LE geometry at R_{NH} = 1.06 Å (structure 3) and the ^{1}CT geometry at R_{NH} = 1.2 Å (structure 4).

structure of the ground state, which raises the ground-state energy by 3–4 eV (see the $S_0^{(CT)}$ curve in Fig. 4a). It should be noted that the crossing of the ^1L_a and ^{1}CT curves in Fig. 4a is an apparent crossing (since these energy profiles correspond to separately optimized reaction paths), while the crossing of the ^{1}CT and $S_0^{(CT)}$ curves is a real crossing (conical intersection).

The ^{1}CT and S_0 energy profiles are surprisingly smooth in the vicinity of the ^{1}CT–S_0 conical intersection, although the ADC(2) method, being a single-reference perturbative method, should break down near degeneracies of excited states with the ground state. The biradical character of the ^{1}CT state may be the explanation of this result. The half-filled molecular orbitals of this state are very different from the HOMO and LUMO orbitals of the ground-state configuration. As a result, the interaction of the ^{1}CT and S_0 configurations is presumably rather small. A detailed characterization of the ^{1}CT–S_0 intersection, in particular the determination of the branching-space vectors, requires the use of MCSCF or MRCI methods.

3.5. Linearly interpolated transit paths

In order to obtain further information on curve crossings among the excited states, we calculated LITPs between different optimized excited-state structures, as indicated in Fig. 4b which gives an enlarged view of the excited-state crossing region in Fig. 4a. The linear transit path connecting the structures 1 and 2 (see Fig. 4b) is denoted as path A. The corresponding energy profiles are shown

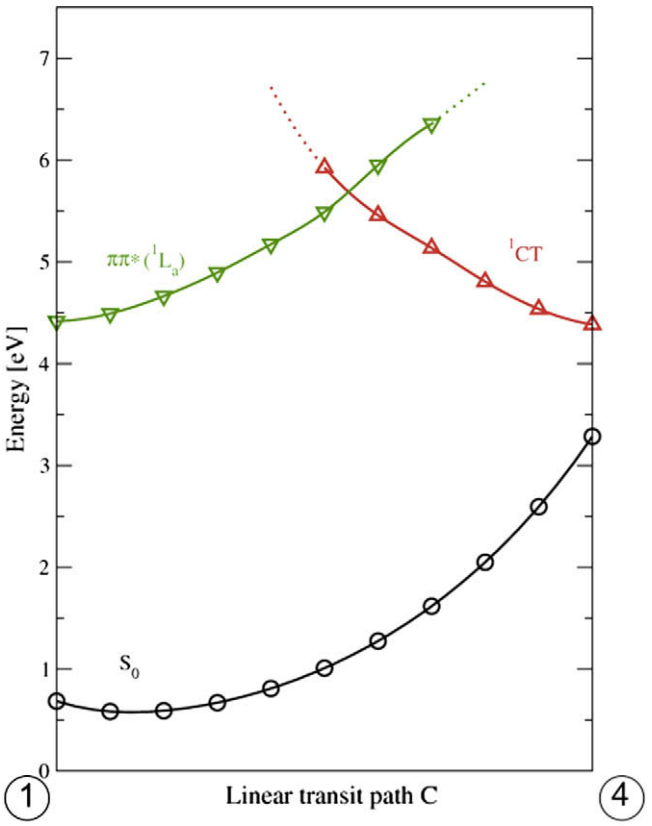


Fig. 7. Potential-energy profiles of the ^1L_a, ^1CT and S_0 states along the linearly interpolated transit path between the ^1L_a minimum-energy geometry (structure 1) and the ^1CT minimum-energy geometry at R_{NH} = 1.2 Å (structure 4).

in Fig. 6a. Path A (see Fig. 6a) connects the ^1L_a energy minimum with the energy minimum of the ^1LE state. At the ^1L_a equilibrium geometry, the ^1LE state lies 1.65 eV above the ^1L_a state. Along path A, the ^1LE and ^1L_a energies cross. The crossing lies approximately 0.7 eV above the energy of the ^1L_a state at the beginning of path A. The barrier associated with the ^1LE–^1L_a crossing is about 0.2 eV higher than the vertical excitation energy of the ^1L_b state.

Path B (see Fig. 6b) connects the equilibrium geometry of the ^1LE state (structure 3) with structure 4 on the ^1CT reaction path. The energy crossing along this path lies about 0.9 eV above the ^1LE energy at the starting configuration. This point is only about 0.15 eV higher than the vertical excitation energy of the ^1L_b state. Path C connects the ^1L_a equilibrium geometry (structure 1) with geometry 4 on the ^1CT relaxed scan, which is almost isoenergetic. The corresponding energy profiles are shown in Fig. 7. It is seen that the ^1L_a–^1CT crossing occurs at a much higher energy than found for the previous paths. The barrier associated with the intersection is about 1.3 eV higher than the energy of the starting configuration, and about 0.85 eV higher than the vertical excitation energy of the ^1LE state.

It should be kept in mind that the paths A, B and C are not minimum-energy paths. The energy crossings in Figs. 6 and 7 are thus upper limits for the true barriers involved in the photochemical dynamics.

4. Discussion of reaction mechanisms

Figs. 3, 4, 6 and 7 provide the quantitative basis for the following qualitative mechanistic picture: Assuming absorption of a UV photon near the absorption threshold of Trp-Gly, the system is vertically excited to the ^1L_b state. This state is strongly vibronically coupled with the ^1L_a state. The ^1L_b and ^1L_a states are nearly degenerate in the Franck–Condon region and the oscillator strengths and dipole moments indicate a profound mixing of the ^1L_a and ^1L_b states. Relaxation to the minimum of the ^1L_a surface yields an enthalpy gain of 0.45 eV. From the ^1L_a state, a radiationless transition to the ^1LE state is possible via a low barrier (<0.2 eV relative to the ^1L_b vertical excitation energy) on path A, see Fig. 6a. From the ^1LE state, another radiationless transition via a low barrier (<0.15 eV relative to the ^1L_b vertical excitation energy) can lead to the ^1CT state on path B, see Fig. 6b. The ^1CT state in turn leads in a barrierless manner to a low-lying conical intersection with the electronic ground state, see Fig. 4a. A direct nonadiabatic transition from the ^1L_a state to the ^1CT state (path C) appears less likely, since a much higher barrier has to be overcome, see Fig. 7. When the system is back in the S_0 state, a considerable energy is released by the back-transfer of the proton to the carboxyl group. By this sequence of radiationless transitions, the energy deposited by the UV photon is converted into vibrational energy in the electronically stable S_0 state. This mechanism enhances the photostability of the dipeptide, since potentially deleterious photochemical reactions are quenched by the ultrafast internal conversion to the ground state.

5. Conclusions

We have investigated possible mechanisms for ultrafast excited-state deactivation of the wg[g+.0.70] conformer of the Trp-Gly dipeptide. The strong hydrogen bond involving the terminal carboxyl group and the CO group of the backbone plays an essential role in the radiationless decay process. The proposed mechanism provides an explanation for the short excited-state lifetime of this specific conformer and thus the lack of a REMPI signal. The rather detailed mechanistic picture is the following: The chromophore is vertically excited to the strongly mixed ^1L_b and ^1L_a states. Low-energy curve crossings of the ^1L_a state with the lowest locally excited state of the backbone (^1LE) and of the latter state with a charge-transfer state (^1CT) of the backbone provide access to a conical intersection of the ^1CT with the electronic ground state. By this sequence of nonadiabatic transitions, the electronic excitation energy is converted into vibrational energy. This mechanism explains why certain conformers, namely those with a strong intramolecular hydrogen bond, have a very short excited-state lifetime and therefore cannot be detected in the REMPI spectrum. The present findings, together with recent results for in the Gly-Phe-Ala tripeptide [17], indicate that ultrafast excited-state deactivation via photoinduced electron- and proton transfer along intramolecular hydrogen bonds is a generic process in peptides and proteins. The highly efficient radiationless deactivation of excited states may play an essential role for the photostability of these biological molecules.

Acknowledgements

This work has been supported by the Deutsche Forschungsgemeinschaft through the DFG cluster of excellence 'Munich-Centre for Advanced Photonics'. D.S. acknowledges support by a research fellowship of the Alexander von Humboldt foundation. A substantial amount of computing time on the Höchstleistungsrechner in Bayern (HLRB) has been provided by the Leibniz-Rechenzentrum der Bayerischen Akademie der Wissenschaften.

References

[1] M.F. Masman, S. Lovas, R.F. Murphy, R.D. Enriz, A.M. Rodriguez, J. Phys. Chem. A 111 (2007) 10682.
[2] N. Doslic, G. Kovacevic, I. Ljubic, J. Phys. Chem. A 111 (2007) 8650.
[3] V. Brenner, F. Piuzzi, I. Dimicoli, B. Tardivel, M. Mons, Angew. Chem. Int. Edit. 46 (2007) 2463.

[4] W. Chin, F. Piuzzi, I. Dimicoli, M. Mons, Phys. Chem. Chem. Phys. 8 (2006) 1033.
[5] H. Valdes, D. Reha, P. Hobza, J. Phys. Chem. B 110 (2006) 6385.
[6] I. Compagnon, J. Oomens, G. Meijer, G. von Helden, J. Am. Chem. Soc. 128 (2006) 3592.
[7] W. Chin, J.P. Dognon, F. Piuzzi, B. Tardivel, I. Dimicoli, M. Mons, J. Am. Chem. Soc. 127 (2005) 707.
[8] W. Chin et al., J. Phys. Chem. A 109 (2005) 5281.
[9] J.M. Bakker et al., Chem. Phys. Chem. 6 (2005) 120.
[10] W. Chin et al., J. Chem. Phys. 122 (2005) 054317.
[11] D. Reha, H. Valdes, J. Vondrasek, P. Hobza, A.G. Abo-Riziq, B.O. Crews, M.S. de Vries, Chem-Eur. J. 11 (2005) 6803.
[12] I. Hünig, K. Kleinermanns, Phys. Chem. Chem. Phys. 6 (2004) 2650.
[13] M. Gerhards, C. Unterberg, A. Gerlach, A. Jansen, Phys. Chem. Chem. Phys. 6 (2004) 2682.
[14] Z. Wang, C. Wu, H. Lei, Y. Duan, J. Chem. Theory Comput. 3 (2007) 1527.
[15] T.K. Harris, A.S. Mildvan, Proteins 35 (1999) 275.
[16] A.L. Sobolewski, W. Domcke, Chem. Phys. Chem. 7 (2006) 561.
[17] D. Shemesh, A.L. Sobolewski, W. Domcke, J. Am. Chem. Soc. 132 (2009) 1374.
[18] C. Hättig, Adv. Quantum Chem. 50 (2005) 37.
[19] A.B. Trofimov, J. Schirmer, J. Phys. B-At. Mol. Opt. Phys. 28 (1995) 2299.
[20] A.B. Trofimov, J. Schirmer, Chem. Phys. 214 (1997) 153.
[21] A.B. Trofimov, J. Schirmer, Chem. Phys. 224 (1997) 175.
[22] J. Schirmer, Phys. Rev. A 26 (1982) 2395.
[23] O. Christiansen, H. Koch, P. Jorgensen, Chem. Phys. Lett. 243 (1995) 409.
[24] C. Hättig, F. Weigend, J. Chem. Phys. 113 (2000) 5154.
[25] A. Köhn, A. Tajti, J. Chem. Phys. 127 (2007) 044105.
[26] R. Ahlrichs, M. Bär, M. Häser, H. Horn, C. Kölmel, Chem. Phys. Lett. 162 (1989) 165.
[27] F. Weigend, M. Häser, Theor. Chem. Acc. 97 (1997) 331.
[28] C.L. Perrin, J.B. Nielson, Annu. Rev. Phys. Chem. 48 (1997) 511.
[29] L. Sobczyk, S.J. Grabowski, T.M. Krygowski, Chem. Rev. 105 (2005) 3513.
[30] B.C. Dian, A. Longarte, T.S. Zwier, J. Chem. Phys. 118 (2003) 2696.
[31] A.L. Sobolewski, W. Domcke, J. Phys. Chem. A 111 (2007) 11725.